

Investigation of sodium borohydride oxidation on CoB/Cu and CoBW/Cu modified with Au nanoparticles

Zita Sukackienė*,

Aldona Balčiūnaitė,

Loreta Tamašauskaitė-Tamašiūnaitė,

Algirdas Selskis,

Vitalija Jasulaitienė,

Eugenijus Norkus

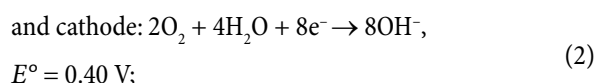
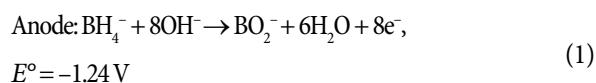
*Institute of Chemistry,
Center for Physical Sciences and Technology,
A. Goštauto St. 9, LT-01108 Vilnius, Lithuania*

The Au/CoB and Au/CoBW catalysts were deposited on the copper surface via electroless CoB and CoBW coating deposition followed by a spontaneous galvanic Au displacement from the HAuCl_4 solution. The morphology and composition of the prepared catalysts were characterized using Field-Emission Scanning Electron Microscopy, Energy Dispersive X-ray Spectroscopy and X-ray Photoelectron Spectroscopy. The electrochemical behaviour of the fabricated Au/CoB/Cu and Au/CoBW/Cu catalysts was examined towards the oxidation of BH_4^- ions in an alkaline medium by means of Cyclic Voltammetry. The as-prepared Au/CoB/Cu and Au/CoBW/Cu catalysts exhibited a higher electrocatalytic activity towards the oxidation of BH_4^- ions as compared with that of pure Au, CoB/Cu and CoBW/Cu electrodes. The Au/CoBW/Cu catalyst with the Au loading of $5.8 \mu\text{g cm}^{-2}$ and with deposited Au nanoparticles in size from 7 to 40 nm has the highest mass activity ($\text{mA } \mu\text{g}_{\text{Au}}^{-1}$).

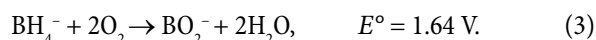
Key words: gold, cobalt, tungsten, copper, galvanic displacement, borohydride oxidation

INTRODUCTION

Fuel cells are alternative energy sources, which allow direct conversion of chemical energy to electric energy [1–3]. One type of fuel cells, the direct borohydride fuel cell (DBFC), operates due to the oxidation of BH_4^- ions at the anode (Eq. (1)) and the reduction of oxygen at the cathode (Eq. (2)):



The overall reaction:



The main benefits of DBFC are high energy density and ease with which sodium borohydride can be stored and transported [4–7].

It is well known that gold is an effective electrocatalyst for the oxidation of BH_4^- ions [8–14], however, the use of a noble metal as an electrode material is limited by its high price. Recent electrochemical studies suggest that alloying Au with transition metals such as Ni [15–19], Co [18–22] and Cu [23, 24] allows reducing its cost and provides better catalytic characteristics for the oxidation of borohydride. It has been determined that bimetallic catalysts usually show a higher activity and stability than the monometallic ones [15, 16, 19, 21, 23, 24]. The main attention is paid to the search of efficient cost-effective catalysts for borohydride oxidation, e. g. precious-metal – non-precious-metal bimetallic or even multi-metallic systems, which allow reducing the content of the expensive material. Nowadays, non-precious systems, such as Ni-Cr [25], Co-W-B [26], Ni/ZnNi/Ni/Cu [27] and CoNiMnB [28], are particularly attractive, however, they have yet to be adequately studied. The authors in Ref. [29, 30] show that the Cu/Ni/AuNi or Ni/PdNi electrodes, prepared by galvanic replacement of Zn by Au or by Pd in the Ni-Zn coating, are also promising anode catalysts for borohydride fuel cells.

In this study we present a simple way for preparation of the gold-cobalt-boron and gold-cobalt-boron-tungsten catalysts with low Au loadings deposited on the copper surface

* Corresponding author. E-mail: zitaja@gmail.com

(denoted as Au/CoB/Cu and Au/CoBW/Cu) via a simple galvanic displacement technique [12] which involves electroless cobalt deposition followed by a spontaneous Au displacement from the HAuCl_4 solution. The morphology and composition of the prepared catalysts were characterized using Field-Emission Scanning Electron Microscopy (FESEM), Energy Dispersive X-ray Spectroscopy (EDX) and X-ray Photoelectron Spectroscopy (XPS). The electrochemical behavior of the fabricated Au/CoB/Cu and Au/CoBW/Cu catalysts was examined towards the oxidation of BH_4^- ions in an alkaline medium by means of Cyclic Voltammetry (CV).

EXPERIMENTAL

Preparation of catalysts

Electroless deposition of the CoB and CoBW coatings was performed on the Cu surface without a prior activation step of the Cu surface with Pd(II) ions. Prior to electroless deposition of Co coatings, Cu substrates (1×1 cm) were pre-treated with 50–100% calcium magnesium oxide, known as “Vienna Lime” (Kremer Pigmente GmbH & Co. KG), and rinsed with deionized water. Then the Cu substrates were placed into the electroless Co plating solutions for various time periods. The CoB coating was deposited on the Cu surface using a solution containing (mol l^{-1}): $\text{CoSO}_4 - 0.05$ and $\text{C}_4\text{H}_8\text{ONH}\cdot\text{BH}_3$ (morpholine borane) $- 0.05$. The bath operated at pH 7 and 30°C . The solution pH was adjusted by addition of 20% NaOH. The deposition time was 90 min. The thickness of the CoB coating was ca. $1 \mu\text{m}$. The film thickness was calculated from the electrode mass difference before and after electroless cobalt deposition using a specific mass value of Co, equal to 8.9 g cm^{-3} .

The CoBW coating was deposited on the Cu surface using a solution containing (mol l^{-1}): $\text{CoSO}_4 - 0.1$, $\text{NH}_2\text{CH}_2\text{COOH} - 0.2$ (glycine), $\text{C}_4\text{H}_8\text{ONH} \cdot \text{BH}_3$ (morpholine borane) $- 0.2$, $\text{Na}_2\text{WO}_4 - 0.003$, $\text{C}_6\text{H}_8\text{O}_7 - 0.0175$ (citric acid). The bath operated at pH 7 and 60°C . Solutions pH was adjusted with 20% NaOH. The deposition time was 30 min. The thickness of the CoBW coating was also ca. $1 \mu\text{m}$.

Au nanoparticles were deposited on the prepared CoB/Cu and CoBW/Cu electrodes by their immersion into a 1 mmol l^{-1} $\text{HAuCl}_4 + 0.1 \text{ mol l}^{-1}$ HCl solution at 25°C for 0.5, 1 and 5 min. The surface-to-volume ratio was $2 \text{ dm}^2 \text{ l}^{-1}$. Then, the fabricated catalysts were used for sodium borohydride electro-oxidation measurements without any further treatment.

Characterization of catalysts

The morphology and composition of the fabricated catalysts were characterized using a SEM/FIB workstation Helios Nanolab 650 with an Energy Dispersive X-ray (EDX) spectrometer INCA Energy 350 X-Max 20. The Au metal loading was estimated from the EDX data using the ThinFilmID software.

Elemental analysis of the obtained coatings was investigated by using an ESCALAB MK II spectrometer (VG Scientific, UK) equipped with an Al $\text{K}\alpha$ X-ray radiation source (1486.6 eV) operated at a fixed pass energy of 20 eV . To ob-

tain depth profiles, the samples were etched in the preparation chamber by ionized argon at a vacuum of $5 \cdot 10^{-4} \text{ Pa}$. XPS analyses are given for coatings at depths of 20 and 40 nm .

Electrochemical measurements

All electrochemical measurements were made with a Metrohm Autolab potentiostat (PGSTAT100) using the Electrochemical Software (Nova 1.6.013). A conventional three-electrode electrochemical cell was used for electrochemical measurements. The as-prepared CoB/Cu, CoBW/Cu, Au/CoB/Cu and Au/CoBW/Cu catalysts with a geometric area of 2 cm^2 were employed as working electrodes, an Ag/AgCl electrode was used as a reference and a Pt sheet with a geometric area of 2 cm^2 was used as a counter electrode. An Au-sputtered quartz crystal with a geometric area of 0.636 cm^2 was used as a bare gold electrode. Cyclic voltammograms were recorded in a 1 mol l^{-1} NaOH solution containing 0.05 mol l^{-1} NaBH_4 at a linear potential sweep rate of 10 mV s^{-1} from the stationary E_s value in the anodic direction up to 0.6 V vs Ag/AgCl at a temperature of 25°C . The presented current densities are normalized with respect to the geometric area of catalysts.

RESULTS AND DISCUSSION

The Au/CoB/Cu and Au/CoBW/Cu catalysts were prepared by a two-step process which involves electroless cobalt deposition followed by a spontaneous gold displacement from the HAuCl_4 . The electroless CoB and CoBW layers were used as an underlayer for the formation of an immersion gold overlayer onto the copper surface. The both CoB and CoBW coatings were deposited on the copper surface by using morpholine borane as a reducing agent.

Figure 1 presents FESEM images of the as-prepared CoB/Cu (a), CoBW/Cu (b), Au/CoB/Cu (c), and Au/CoBW/Cu (d) catalysts. As evident from the data in Fig. 1, the CoB coating, deposited on the copper surface, has a structure consisting of larger agglomerates and Co particles of 6 to 25 nm in size (Fig. 1a). The CoBW coating, deposited on the copper surface, consists of a Co layer with crystallites from 110 to 760 nm in size (Fig. 1b). The particles of a CoBW film are larger and almost equilateral as compared with the Co particles.

Immersion of CoB/Cu and CoBW/Cu in the gold-containing solution for 0.5 min results in the formation of Au nanoparticles on the CoB/Cu or CoBW/Cu electrodes (Fig. 1c, d). It is seen that the Au nanoparticles of $6\text{--}50 \text{ nm}$ (Fig. 1c) and $7\text{--}40 \text{ nm}$ (Fig. 1d) in size were deposited on the CoB/Cu and CoBW/Cu electrodes, respectively.

The presence of Au, Co, Cu and W was confirmed by EDX analysis and is summarized in Table 1. Significant amounts of deposited cobalt and much lower amounts of gold remaining on the electrode surface were determined. The Au loadings were 8 and $5.8 \mu\text{g}_{\text{Au}} \text{ cm}^{-2}$ in the as-prepared Au/CoB/Cu and Au/CoBW/Cu catalysts, respectively, after immersion of the CoB/Cu and CoBW/Cu electrodes into 1 mmol l^{-1} HAuCl_4 at 25°C for 0.5 min, respectively.

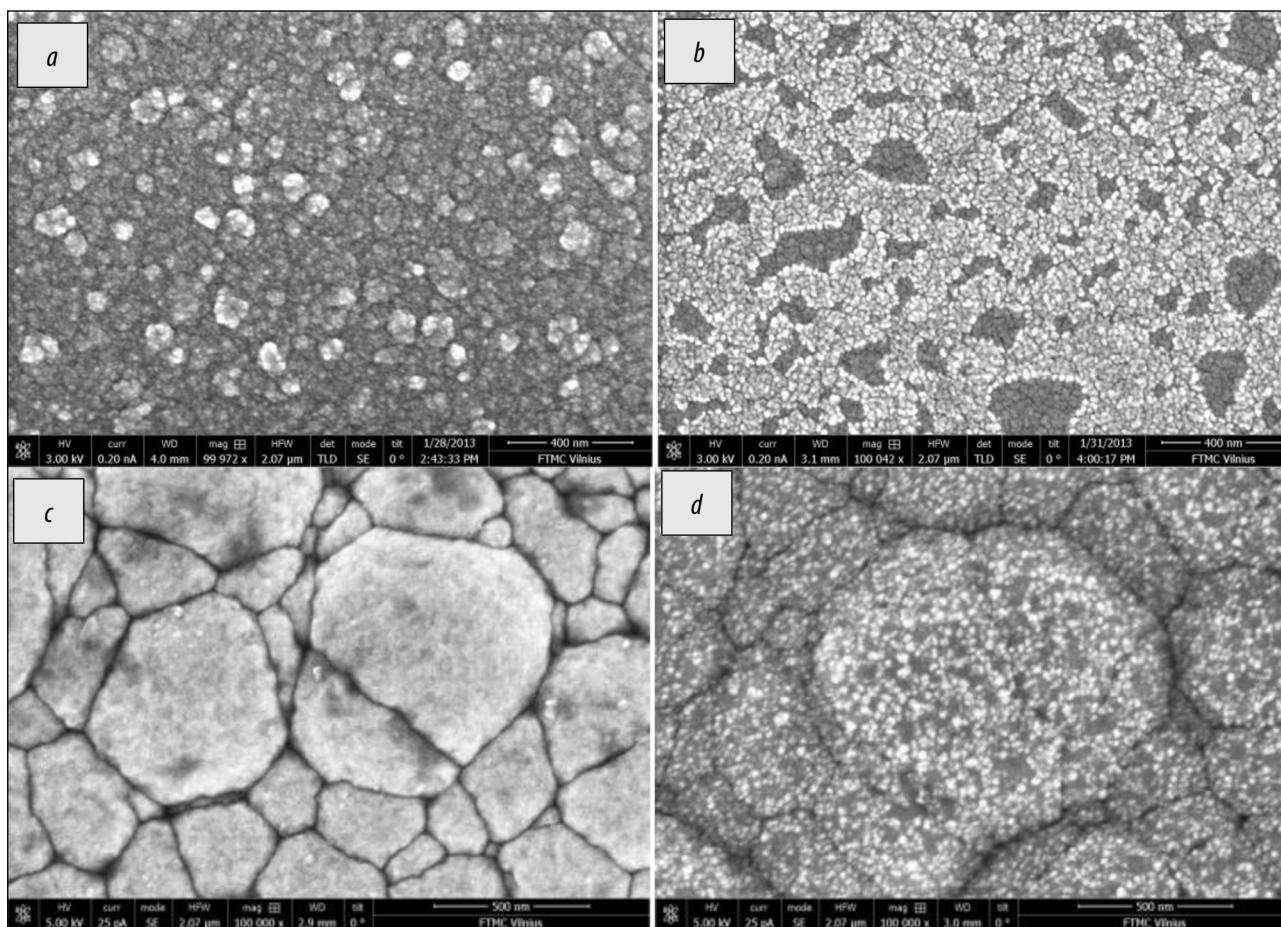


Fig. 1. FESEM images of the as-prepared CoB/Cu (a), CoBW/Cu (b), Au/CoB/Cu (c) and Au/CoBW/Cu (d) catalysts. The Au/CoB/Cu and Au/CoBW/Cu catalysts were prepared by immersion of CoB/Cu and CoBW/Cu into $1 \text{ mmol l}^{-1} \text{ HAuCl}_4 + 0.1 \text{ mol l}^{-1} \text{ HCl}$ at 25°C , respectively, for 0.5 min

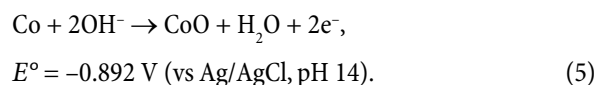
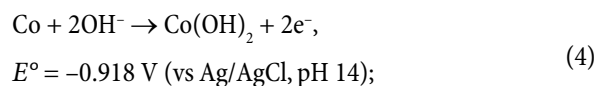
Table 1. Surface atomic composition of the CoB/Cu, CoBW/Cu, Au/CoB/Cu and Au/CoBW/Cu catalysts with the Au loadings of 8.0 and $5.8 \mu\text{g}_{\text{Au}} \text{ cm}^{-2}$, respectively, by EDX analysis. The catalysts are the same as in Fig. 1

Catalysts	Elements, at. %				Size of cobalt particles, nm	Size of gold particles, nm
	Cu	Co	W	Au		
CoB/Cu	3.25	96.75	–	–	6–25	–
CoBW/Cu	3.94	89.79	6.28	–	110–760	–
Au/CoB/Cu	11.77	87.55	–	0.67	–	6–50
Au/CoBW/Cu	3.55	90.11	5.76	0.64	–	7–40

According to the XPS spectral analysis of the CoB coating, the obtained Co coating contained ca. 10.4–13.0 at.% B (Fig. 1a). The CoBW coating obtained has the following composition at a depth of 20 nm: ca. 59.76 at.% of Co, 6 at.% of W and 4 at.% of B at a depth of 40 nm: 66.81 at.% of Co, 8.5 at.% of W and 4 at.% of B (Fig. 1b).

The electrochemical behavior of the CoB/Cu and CoBW/Cu electrodes towards the oxidation of BH_4^- ions was evaluated in an alkaline medium using cyclic voltammetry. Figure 2 presents CVs for the CoB/Cu (a) and CoBW/Cu (b) catalysts

recorded in a $1 \text{ mol l}^{-1} \text{ NaOH}$ solution containing $0.05 \text{ mol l}^{-1} \text{ NaBH}_4$ at 25°C at a scan rate of 10 mV s^{-1} . The insets represent CVs of CoB/Cu (a') and CoBW/Cu (b') in a $1 \text{ mol l}^{-1} \text{ NaOH}$ solution. As seen from the data in Fig. 2 a' and b', anodic peaks **A0** and cathodic peaks **C0** in the reverse scan are seen in the CVs. Anodic peak **A0** may be attributed to the formation of cobalt oxide and hydroxide in an alkaline medium according to the following reactions [31–33]:



Cathodic peaks **C0** may be related with the reactivation of oxidized Co surface during the previous anodic scan, e. g. the reduction of Co oxy/hydroxy compounds to the bare metal (Eqs. (4, 5)).

In the CVs for CoB/Cu (a) and CoBW/Cu (b) catalysts, recorded in an alkaline borohydride solution, two anodic

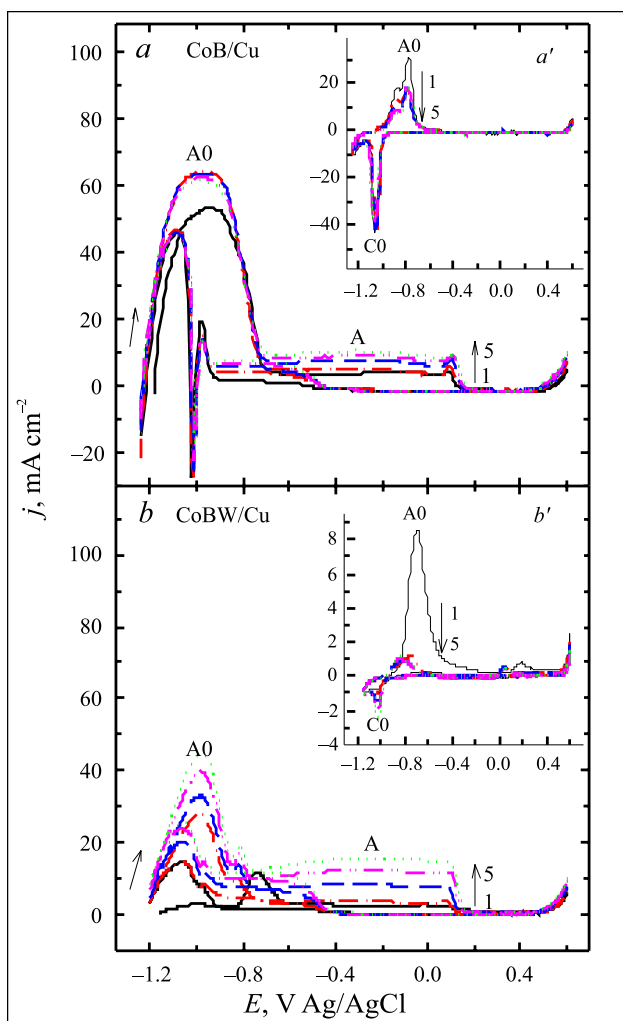


Fig. 2. CVs for CoB/Cu (a) and CoBW/Cu (b) recorded in $0.05 \text{ mol l}^{-1} \text{ NaBH}_4 + 1 \text{ mol l}^{-1} \text{ NaOH}$ (a, b) at 10 mV s^{-1} at $25 \text{ }^\circ\text{C}$. The insets (a') and (b') represent the CVs of CoB/Cu (a') and CoBW/Cu (b') in $1 \text{ mol l}^{-1} \text{ NaOH}$. The number of scans: 1st – solid line, 2nd – dash-dotted line, 3rd – dashed line, 4th – dash-dot-dotted line and 5th – dotted line

peaks **A0** and **A** are recorded in contrast to the CVs recorded at both catalysts in a $1 \text{ mol l}^{-1} \text{ NaOH}$ solution (Fig. 2). Anodic peak **A0** recorded at lower potential values may be related with the oxidation of hydrogen generated by sodium borohydride hydrolysis. The second peak **A** at more positive potential values may be ascribed to direct oxidation according to Eq. (1).

Figure 3 presents continuous CVs of bare Au (a), Au/CoB/Cu (b) and Au/CoBW/Cu (c) catalysts in an alkaline borohydride solution. It is well known that gold is an effective electrocatalyst for the oxidation of BH_4^- ions [8, 10, 34–36] indicating that the anodic oxidation of BH_4^- ions at the gold electrode proceeds through an eight-electron process according to Eq. (1), assuming that hydrolysis does not occur. As seen from the data in Fig. 3a, in the positive potential scan a broad anodic peak **A** is observed at a potential of -0.4 V vs Ag/AgCl. This oxidation peak is attributed to the direct oxidation of BH_4^- ions according to Eq. (1). Furthermore, a wide

oxidation wave that extends up to 0.4 V corresponds to the oxidation of reaction intermediates on a partially oxidized Au surface [35]. In the reverse scan, a sharp peak **B** is observed at ca. 0.2 V followed by a plateau in the potential region from 0 to -0.6 V . This peak corresponds to the oxidation of adsorbed species such as BH_3OH^- or other borohydrides formed as an intermediate during the oxidation of the BH_4^- ion in the forward scan [35]. But recent findings by the authors in [37, 38]

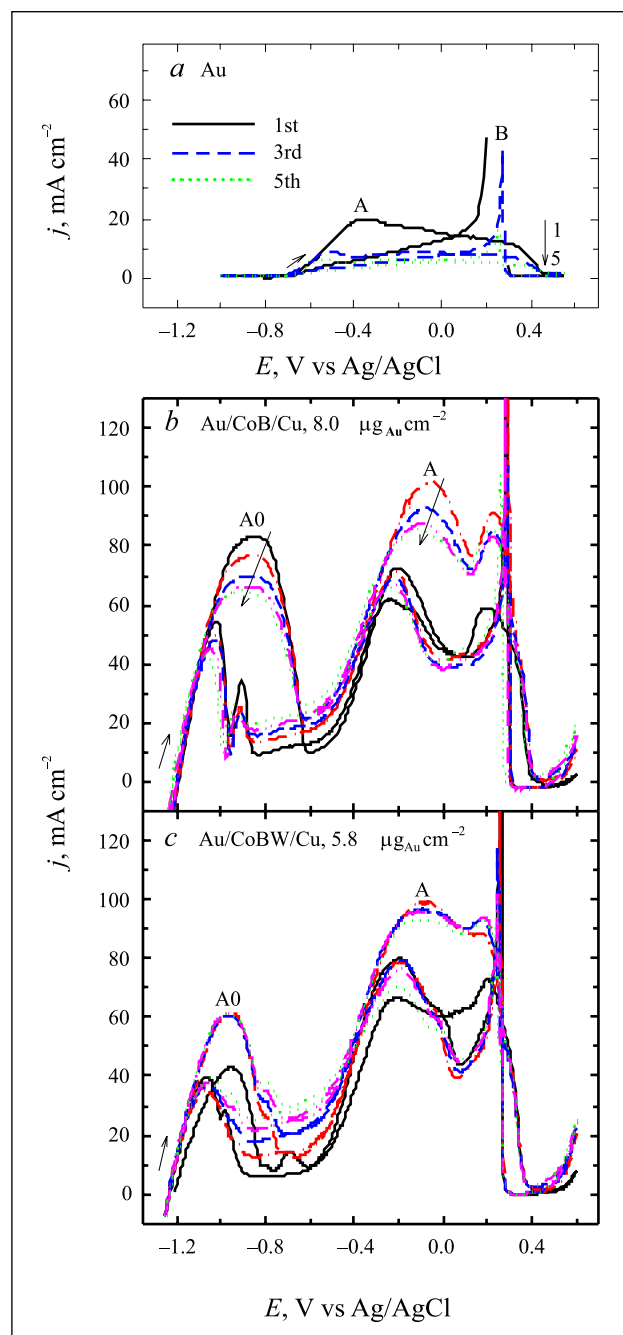


Fig. 3. CVs for Au (a), Au/CoB/Cu (b) and Au/CoBW/Cu (c) recorded in $0.05 \text{ mol l}^{-1} \text{ NaBH}_4 + 1 \text{ mol l}^{-1} \text{ NaOH}$ at 10 mV s^{-1} . Au/CoB/Cu and Au/CoBW/Cu were prepared by immersion of CoB/Cu and CoBW/Cu into $1 \text{ mmol l}^{-1} \text{ HAuCl}_4 + 0.1 \text{ M HCl}$ at $25 \text{ }^\circ\text{C}$, respectively, for 0.5 min . The number of scans: 1st – solid line, 2nd – dash-dotted line, 3rd – dashed line, 4th – dash-dot-dotted line and 5th – dotted line

show that gold is not a fully faradaic-efficient electrocatalyst for the oxidation of borohydride. It was found that during the oxidation of borohydride on the gold electrode, generation of H_2 was monitored over a wide potential range, indicating that gold also serves as a catalyst for the catalytic decomposition of BH_4^- , e. g. gold is not inert towards the hydrolysis reaction [37]. The formation of BH_3OH^- was determined during borohydride oxidation on a gold electrode in an alkaline solution by means of rotating-disc electrode voltammetry [39]. The presence of BH_3OH^- and related species on the Au surface was also confirmed by FTIR spectroscopy at open circuit and low anodic over potentials [40] and EQCM measurements [41].

In the case of Au/CoB/Cu and Au/CoBW/Cu, during the anodic scan in contrast to borohydride oxidation on the bare Au electrode, two anodic peaks are seen in the CVs plots. Anodic peak **A0** seen in the CVs for Au/CoB/Cu and Au/CoBW/Cu catalysts may be related with the oxidation of hydrogen generated by sodium borohydride hydrolysis. The second peak **A** may be ascribed to direct borohydride oxidation as it appears in the same potential region as on bare Au (Fig. 3). It should be noted that the both oxidation peaks **A0** and **A** recorded on Au/CoB/Cu and Au/CoBW/Cu are higher than those on CoB/Cu and CoBW/Cu (Fig. 2). As seen from the data in Fig. 3, higher borohydride oxidation current densities (peak **A**) were obtained at Au/CoB/Cu and Au/CoBW/Cu as compared to those at the bare Au electrode, indicating a high activity of the Au/CoB/Cu and Au/CoBW/Cu catalysts.

During long-term cycling, the anodic current densities recorded at AuCoB/Cu are decreased (Fig. 3b), whereas the values of anodic current densities obtained at AuCoBW/Cu are very close (Fig. 3c).

Figure 4a presents the comparison of stabilized positive-potential going scans (5th) of the oxidation of BH_4^- ions recorded on the bare Au (1), CoB/Cu (2), CoBW/Cu (3) Au/CoB/Cu (4), Au/CoBW/Cu (5) catalysts at a potential scan rate of 10 mV s^{-1} . It is evident that both oxidations peaks **A0** and **A** are significantly higher on Au/CoB/Cu and Au/CoBW/Cu with the Au loadings of 8 and $5.8 \mu\text{g cm}^{-2}$ than those on bare Au or CoB/Cu and CoBW/Cu (Fig. 4a). An enhanced activity of the Au/CoB/Cu and Au/CoBW/Cu catalysts can be ascribed to the intrinsic electrocatalytic activity of the Au particles deposited on the CoB/Cu and CoBW/Cu electrodes [18, 20, 21].

To compare the electrocatalytic activity of the Au/CoB/Cu and Au/CoBW/Cu catalysts, the current density values were normalized in reference to the Au loadings for each catalyst and are given in Fig. 4b. The Au/CoBW/Cu catalyst with the Au loading of $5.8 \mu\text{g cm}^{-2}$ and with deposited Au nanoparticles 7 to 40 nm in size has the highest mass activity ($\text{mA } \mu\text{g}_{\text{Au}}^{-1}$) for the both oxidation peaks **A0** and **A**. The mass activities for anodic peaks **A0** and **A** are ca. 1.3 and 1.5, respectively, higher on the Au/CoBW/Cu catalyst as compared with those on the Au/CoB/Cu catalyst.

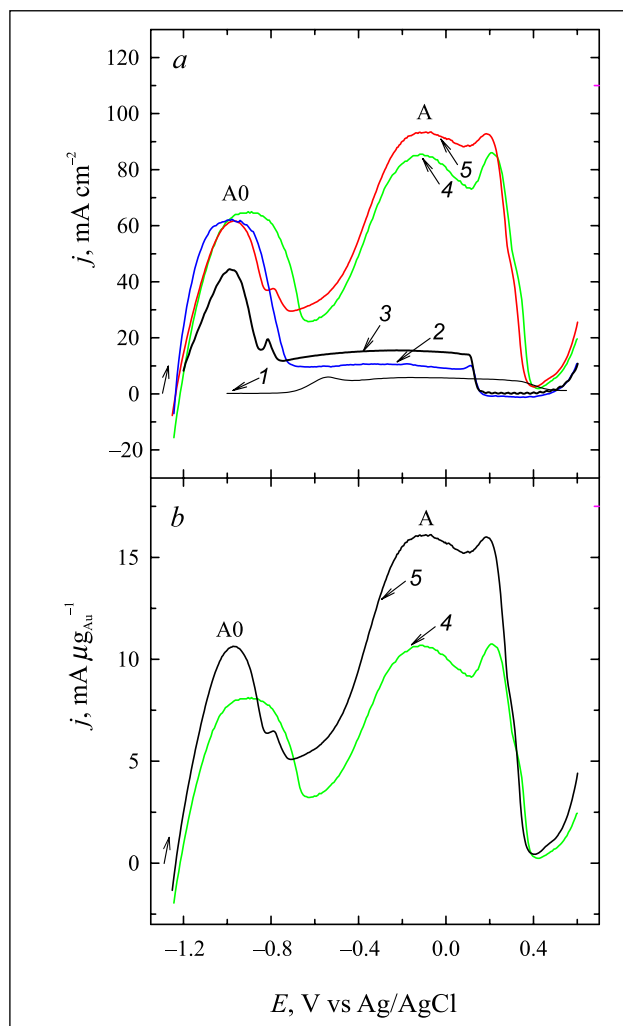


Fig. 4. (a) Stabilized positive-potential going scans (5th) of the Au (1), CoB/Cu (2), CoBW/Cu (3), Au/CoB/Cu (4) and Au/CoBW/Cu (5), recorded in $0.05 \text{ mol l}^{-1} \text{ NaBH}_4 + 1 \text{ mol l}^{-1} \text{ NaOH}$ at 10 mV s^{-1} . The catalysts are the same as in Fig. 3. (b) The same data are normalized by the Au loadings

The Au/CoB/Cu and Au/CoBW/Cu catalysts with different Au loadings were prepared by immersion of CoB/Cu and CoBW/Cu into a $1 \text{ mmol l}^{-1} \text{ HAuCl}_4 + 0.1 \text{ mol l}^{-1} \text{ HCl}$ solution at $25 \text{ }^\circ\text{C}$ for 0.5, 1 and 5 min. Figure 5 presents bar plots of borohydride oxidation current densities under both anodic peaks **A0** (a) and **A** (b) recorded at the prepared different Au/CoB/Cu and Au/CoBW/Cu and normalized by the Au loadings for each catalyst. Voltammetric characteristics of borohydride oxidation for the Au, CoB/Cu, CoBW/Cu and different Au/CoB/Cu and Au/CoBW/Cu catalysts are given in Table 2. As seen from the data in Fig. 5, the Au/CoBW/Cu catalysts with the Au loadings in the range 5.8 to $23.2 \mu\text{g cm}^{-2}$ exhibit the highest mass activities ($\text{mA } \mu\text{g}_{\text{Au}}^{-1}$) as compared to those of the Au/CoB/Cu catalysts with the Au loadings in the range 8 to $44.2 \mu\text{g cm}^{-2}$. The Au/CoBW/Cu catalyst with the Au loading of $5.8 \mu\text{g cm}^{-2}$ and with deposited Au nanoparticles 7 to 40 nm in size has the highest mass activity for the both oxidation peaks **A0** and **A**.

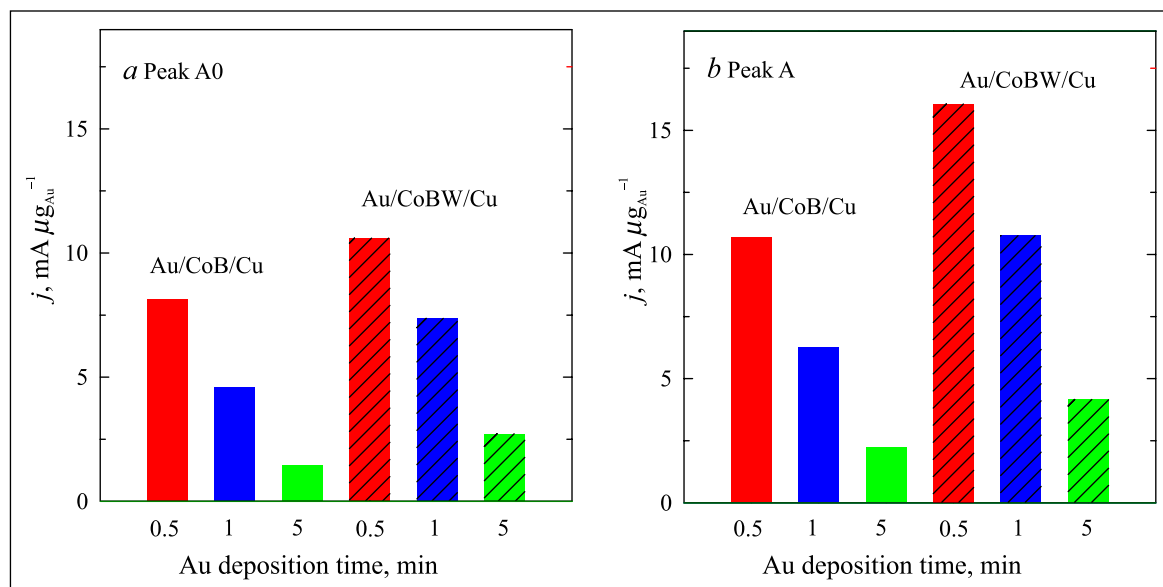


Fig. 5. Bar plots of BH_4^- oxidation current densities normalized by the Au loadings for each catalyst obtained on Au/CoB/Cu and Au/CoBW/Cu at a potential of peaks **A0** (a) and **A** (b). The Au/CoB/Cu and Au/CoBW/Cu catalysts were prepared by immersion of CoB/Cu and CoBW/Cu into $1 \text{ mmol l}^{-1} \text{ HAuCl}_4 + 0.1 \text{ mol l}^{-1} \text{ HCl}$ at 25°C , respectively, for 0.5 min (red), 1 min (blue) and 5 min (green)

Table 2. Voltammetric characteristics of borohydride oxidation for Au (1), CoB/Cu (2), CoBW/Cu (6) and different Au/CoB/Cu (3–5) and Au/CoBW/Cu (7–9) catalysts

No.	Catalysts	Au deposition time, min	Au loading, $\mu\text{g cm}^{-2}$	Peak A0		Peak A	
				j , mA cm^{-2}	j , $\text{mA } \mu\text{g}_{\text{Au}}^{-1}$	j , mA cm^{-2}	j , $\text{mA } \mu\text{g}_{\text{Au}}^{-1}$
1.	Au	–	–	–	–	–	–
2.	CoB/Cu	–	–	62.20	–	10.70	–
3.	Au/CoB/Cu	0.5	8.0	65.00	8.12	85.50	10.69
4.	Au/CoB/Cu	1.0	14.3	65.75	4.60	89.65	6.27
5.	Au/CoB/Cu	5.0	44.2	64.40	1.46	97.85	2.21
6.	CoBW/Cu	–	–	44.51	–	15.52	–
7.	Au/CoBW/Cu	0.5	5.8	61.71	10.60	93.47	16.06
8.	Au/CoBW/Cu	1.0	7.6	56.11	7.36	81.95	10.75
9.	Au/CoBW/Cu	5.0	23.2	63.09	2.71	96.53	4.16

CONCLUSIONS

In this study we have successfully prepared the Au/CoB/Cu and Au/CoBW/Cu catalysts with low Au loadings by a simple way which involves electroless CoB and CoBW deposition on the copper surface followed by a spontaneous Au displacement from the gold-containing solution. It has been determined that the average size of Au crystallites deposited by galvanic displacement of CoB and CoBW adlayers varies from 6 up to 50 nm. The prepared Au/CoB/Cu and Au/CoBW/Cu catalysts with low Au loadings demonstrated a significantly higher electrocatalytic activity towards the oxidation of H_2 generated by catalytic hydrolysis of BH_4^- and the oxidation of BH_4^- ions as compared to those of bare Au, CoB/Cu or CoBW/Cu.

The Au/CoBW/Cu catalyst with the Au loading of $5.8 \mu\text{g cm}^{-2}$ and with deposited Au nanoparticles in size from 7 to 40 nm has the highest mass activity ($\text{mA } \mu\text{g}_{\text{Au}}^{-1}$).

Received 26 March 2015

Accepted 27 April 2015

References

1. J. Larminie, A. Dicks, *Fuel Cell Systems Explained*, 2nd edn., John Wiley & Sons Ltd., 433 (2003).
2. C. Rayment, S. Sherwin, *Introduction to Fuel Cell*, University of Notre Dame, USA, 156 (2003).
3. *Fuel Cell Handbook*, 7th edn., EG & G Technical Services, Inc., Morgantown, West Virginia, 427 (2004).

4. S. C. Amendola, P. Onnerud, M. T. Kelly, P. J. Petillo, S. L. Sharp-Goldman, M. Binder, *J. Power Sources*, **84**, 130 (1999).
5. C. P. de Leon, F. C. Walsh, D. Pletcher, D. J. Browning, J. B. Lakeman, *J. Power Sources*, **155**, 172 (2006).
6. C. Celik, San F. G. Boyaci, H. I. Sarac, *J. Power Sources*, **185**, 197 (2008).
7. C. Celik, San F. G. Boyaci, H. I. Sarac, *J. Power Sources*, **195**, 599 (2010).
8. K. Wang, J. Lu, L. Zhuang, *J. Electroanal. Chem.*, **585**, 191 (2005).
9. M. H. Atwan, C. L. B. Macdonald, D. O. Northwood, E. L. Gyenge, *J. Power Sources*, **158**, 36 (2006).
10. M. Chatenet, F. Micoud, I. Roche, E. Chainet, *Electrochim. Acta*, **51**, 5459 (2006).
11. G. Rostamika, M. Janic, *J. Electrochem. Soc.*, **156**, B86 (2009).
12. J. Wei, X. Wang, Y. Wang, Q. Chena, F. Pei, Y. Wang, *Int. J. Hydrogen Energy*, **34**, 3360 (2009).
13. D. M. F. Santos, C. A. C. Sequeira, *Electrochim. Acta*, **55**, 6775 (2010).
14. D. M. F. Santos, C. A. C. Sequeira, *Renew. Sustain. Energy Rev.*, **15**, 3980 (2011).
15. D. Cao, Y. Gao, G. Wang, R. Miao, Y. Liu, *Int. J. Hydrogen Energy*, **35**, 807 (2010).
16. L. Tamašauskaitė-Tamašiūnaitė, A. Balčiūnaitė, D. Šimkūnaitė, A. Selskis, *J. Power Sources*, **202**, 85 (2012).
17. L. Tamašauskaitė-Tamašiūnaitė, A. Balčiūnaitė, R. Čekavičiūtė, A. Selskis, *J. Electrochem. Soc.*, **159**, B611 (2012).
18. P. He, X. Wang, Y. Liu, X. Liu, L. Yi, *Int. J. Hydrogen Energy*, **37**, 11984 (2012).
19. R. L. Arevalo, M. C. S. Escano, A. Y.-S. Wang, H. Kasai, *Dalton Trans.*, **42**, 770 (2013).
20. F. Pei, Y. Wang, X. Wang, et al., *Int. J. Hydrogen Energy*, **35**, 8136 (2010).
21. L. Tamašauskaitė-Tamašiūnaitė, A. Jagminienė, A. Balčiūnaitė, et al., *Int. J. Hydrogen Energy*, **38**, 14232 (2013).
22. Z. Sukackienė, A. Balčiūnaitė, L. Tamašauskaitė-Tamašiūnaitė, V. Pakštas, A. Selskis, E. Norkus, *ECS Trans.* **59**(1), 295 (2014).
23. L. Yi, Y. Song, X. Liu, et al., *Int. J. Hydrogen Energy*, **36**, 15775 (2011).
24. L. Tamašauskaitė-Tamašiūnaitė, A. Balčiūnaitė, A. Zabielaitė, et al., *J. Electroanal. Chem.*, **700**, 1 (2013).
25. D. M. Yu, Y. Shen, Z. Ye, J. Z. Wen, J. Wang, C. G. Chen, *Chin. Sci. Bull.*, **58**, 2435 (2013).
26. S. Li, X. Yang, H. Zhu, X. Wei, Y. Liu, *Int. J. Hydrogen Energy*, **38**, 2884 (2013).
27. M. G. Hosseini, M. Abdolmaleki, S. Ashrafpoor, *Chin. J. Catal.*, **33**, 1817 (2012).
28. M. Mitov, G. Hristov, E. Hristova, R. Rashkov, M. Arnautova, A. Zielonka, *Environ. Chem. Lett.*, **7**, 167 (2009).
29. M. G. Hosseini, M. Abdolmaleki, F. Nasirpour, *Electrochim. Acta*, **114**, 215 (2013).
30. M. G. Hosseini, M. Abdolmaleki, *Int. J. Hydrogen Energy*, **38**, 5449 (2012).
31. E. Juzeliūnas, S. Lichušina, Patent of the Republic of Lithuania No. 5481, 26.03.2008.
32. W. K. Bell, J. E. Toni, *J. Electroanal. Chem.*, **31**, 63 (1971).
33. L. D. Burke, M. E. Lyons, O. J. Murphy, *J. Electroanal. Chem.*, **132**, 247 (1982).
34. L. D. Burke, M. M. Murphy, *J. Electrochem. Soc.*, **138**, 88 (1991).
35. E. Gyenge, *Electrochim. Acta*, **49**, 965 (2004).
36. H. Cheng, K. Scott, *Electrochim. Acta*, **51**, 3429 (2006).
37. M. Chatenet, F. H. B. Lima, E. A. Ticianelli, *J. Electrochem. Soc.*, **157**, B697 (2010).
38. F. H. B. Lima, A. M. Pasqualetti, M. B. Molina Concha, M. Chatenet, E. A. Ticianelli, *Electrochim. Acta*, **84**, 202 (2012).
39. P. Krishan, T.-H. Yang, S. G. Advani, A. K. Prasad, *J. Power Sources*, **182**, 106 (2008).
40. B. Molina Concha, M. Chatenet, C. Coutanceau, F. Hahn, *Electrochem. Comm.*, **11**, 223 (2009).
41. A. Igaszak, D. C. W. Kannangara, V. W. S. Lam, L. Gyenge, *J. Electrochem. Soc.*, **160**, H47 (2013).

**Zita Sukackienė, Aldona Balčiūnaitė,
Loreta Tamašauskaitė-Tamašiūnaitė, Algirdas Selskis,
Vitalija Jasulaitienė, Eugenijus Norkus**

NATRIO TETRAHIDROBORATO OKSIDACIJOS TYRIMAS ANT Au NANODALELĖMIS MODIFIKUOTŲ CoB/Cu IR CoBW/Cu KATALIZATORIŲ

S a n t r a u k a

Darbo metu Au nanodalelėmis modifikuoti CoB/Cu ir CoBW/Cu katalizatoriai buvo suformuoti taikant paprastus ir nesudėtingus cheminio metalų nusodinimo bei galvaninio pakeitimo metodus. CoB ar CoBW pasluoksnis buvo nusodintas ant vario elektrodo taikant auto-katalizinę Co (II) jonų redukciją, reduktoriais naudojant morfolino boraną. Au nanodalelės buvo nusodinamos ant CoB/Cu ir CoBW/Cu elektrodų, įmerkiant pastaruosius į 1 mmol l⁻¹ HAuCl₄ + 0,1 mol l⁻¹ HCl 25 °C temperatūros tirpalą 0,5, 1 ir 5 min. Gautų katalizatorių morfologija bei struktūra buvo iširta lauko emisijos skenuojančios elektroninės mikroskopijos (LESEM), Rentgeno spindulių energijos dispersinės analizės (EDS) ir Rentgeno fotoelektroninės spektroskopijos (RFES) metodais, o jų elektrokatalizinės savybės įvertintos natrio tetrahidroborato oksidacijos reakcijai taikant ciklinę voltamperometriją. Nustatyta, kad didžiausiu kataliziniu aktyvumu borhidrido oksidacijos reakcijai pasižymėjo Au/CoBW/Cu, kai nusodintų Au dalelių dydis – 7–40 nm, o nusodinto Au įkrova – 5,8 μg cm⁻².